Chemie der Erde 78 (2018) 314–322

Contents lists available at ScienceDirect

Chemie der Erde

journal homepage: www.elsevier.com/locate/chemer

Carbon isotope and REE characteristics of the Paleocene–Eocene shallow marine Subathu formation from the NW Himalaya (India) and their paleoenvironmental implications

Matsyendra Kumar Shukla*, Anupam Sharma

Birbal Sahni Institute of Palaeosciences, 53 University Road, Lucknow, 226 007, U.P., India

ARTICLE INFO

Handling Editor: P.D. Roy

Keywords:
Himalaya
Subathu formation
PETM
$\delta^{13}C$
Ce anomaly

ABSTRACT

Carbon isotope ($\delta^{13}C$) and rare earth element (REE) concentrations in representative samples of the shallow marine Subathu Formation, explored from the Neelkanth and Dogadda sections of Northwestern Himalaya (India) were determined to infer the palaeo-environmental condition during the late Paleocene and middle Eocene. $\delta^{13}C$ values show variation of ~5.0‰ with maximum excursion (−27.34‰) in calcareous sandstone at the basal part and minimum (−22‰) in red shale towards the terminal end. Total REE concentration varies (due to lithology) from 27.23 ppm to 564.35 ppm with an average of 187.60 ppm. The chondrite and PAAS normalized patterns exhibit positive Ce anomaly (0.95–4.45), enriched LREE, and depleted HREE, medium Y/Ho ratio (~30–45) along with positive correlation between Y/Dy and Y/Ho ratio. In addition, calcite veins present in some shale samples indicate redox sensitive trace elements. The overall REE abundance and distribution suggests highly oxygenated environment under the shallow marine regressive phase of deposition. The depositional setting, biostratigraphical constrained age along with $\delta^{13}C$ values and lower TOC suggested an intense warm period, that might be coeval with the Paleocene-Eocene Thermal Maxima event (PETM).

1. Introduction

It is believed that the Paleocene-Middle Eocene shallow marine Subathu Formation of the Northwestern Himalaya was accumulated in a foreland basin that formed after the collision of the India-Asia plate and eventual withdrawal of the Neo-Tethys Sea that occupied the area between these two plates (Batra, 1989; Najman and Garzanti, 2000; Najman et al., 2004; Kumar and Loyal, 2006). It is a valuable archive of collision episodes providing records of the onset of continental sedimentation as a consequence of initial contact with lots of information regarding past geologic and paleo-environmental histories. The Paleogene shallow marine Subathu Formation forms an angular unconformity with the underlying Precambrian basement rocks and it may act as an important archive to understand the well-known event of intense global warming, i.e., Paleocene-Eocene Thermal Maxima (PETM).

There are several stratigraphically correlatable sedimentary sequences distributed along the northwestern and central regions of India formed around the Paleocene-Eocene transitory Epoch (Fig. 1) and the present study area is also one of them. The PETM refers to an important climatic event that lasted for ~170,000 years during the transitory phase of the Paleocene and Eocene (at 55.8 Ma) (Katz et al., 1999; Zachos et al., 2001). It was a critical time in history of the earth, characterized by changes in climate, ocean circulation and evolutionary turnovers and extinctions of marine and terrestrial biota (Crouch et al., 2003). During this event the overall average global temperature increased by ~6 °C, and ~5 °C of it increased in less than 10,000 years (Koch et al., 1995; Zachos et al., 2006, 2008). The global negative Carbon Isotope Excursion (CIE) and a widespread dissolution of seafloor carbonate sediments were the characteristic features of the PETM event that is supposed to be caused by a rapid release of a large mass (above 2000 Gt C) of ^{12}C-enriched and isotopically depleted carbon (Koch et al., 1995; Dickens et al., 2001; Crouch et al., 2003; Smith et al., 2006). The hypotheses for the source(s) and mechanism(s) of such a huge amount of carbon release still remain controversial. However, it is believed that thermal dissociation of marine methane hydrates, widespread oxidation of organic carbon, igneous intrusion into organic-rich sediments, and bolide impact are some of the possible reasons (Bowen et al., 2015). Worldwide studies provide enough evidences of contemporary global temperature rise and it will continue for next several decades (Dickens et al., 2001; Zachos et al., 2008; Bowen et al., 2015). In this situation, understanding of the Paleocene-Eocene global

* Corresponding author.
E-mail address: matsyendra.shukla@gmail.com (M.K. Shukla).

https://doi.org/10.1016/j.chemer.2018.06.005
Received 23 January 2018; Received in revised form 19 June 2018; Accepted 26 June 2018

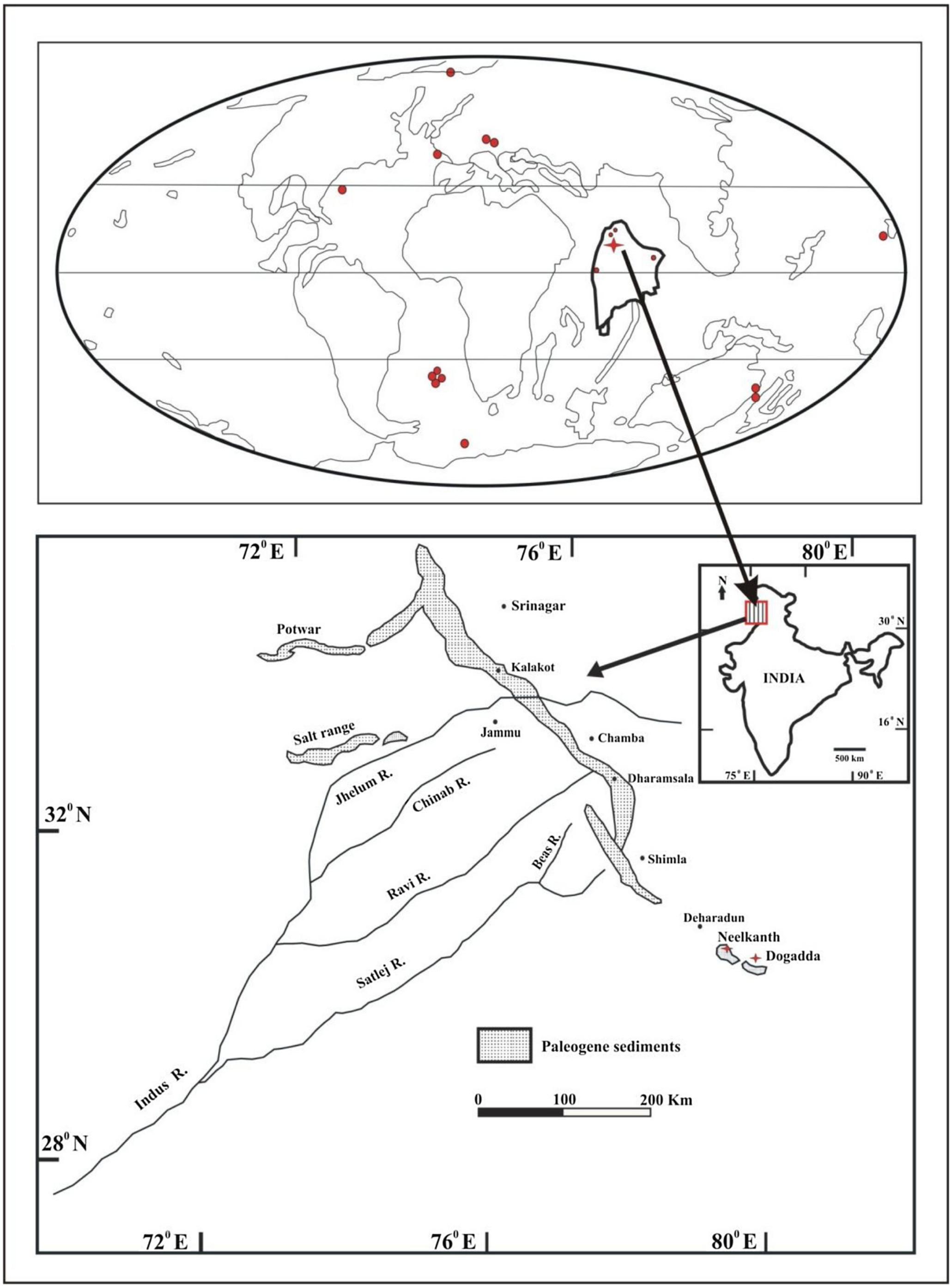

Fig. 1. Dispersion of Paleogene sediments of NW Himalaya, India along with Paleogeographic locations (red circles) of documented PETM sections (modified after Bhatia and Bhargava, 2006 and Samanta et al., 2013) (For interpretation of the references to colour in this figure legend, the reader is referred to the web version of this article).

warming will be useful in interpreting the future global warming.

There are several evidences of PETM event in the present study area (Siva Siddaiah, 2008; Siva Siddaiah and Kumar, 2007; Acharyya, 2007) for example, the shale-dominated Subathu Formation comprised of impersistent coal horizons. The occurrence of the oldest volcanic ash horizon and berthierine-rich ooidal ironstone, however, are some of the important evidences of intense warming that happened during the Paleocene- Eocene (Siva Siddaiah, 2008; Siva Siddaiah and Kumar, 2007; Acharyya, 2007). The berthierine-rich ooidal ironstone discovered within the carbonaceous-shale in lower part of the Subathu Formation (Late Palaeocene-Middle Eocene) indicates a temperature of ~130–160 °C of buried diagenesis of the Dogadda ironstone (Siva Siddaiah, 2008). Base of the Paleogene sequences (late Paleocene) in Jammu area of the NW Himalaya is marked by presence of bauxite deposits (Oxisol) formed in an oxygenated environment (Singh et al., 2009). It is also an indication of warmer condition. Similarly, the coal bearing and stratigraphically equivalent to the east Khasi hill successions of the NE Himalaya portray a PETM connection (Tewari et al., 2010; Srivastava and Prasad, 2015). Additionally, an evidence of volcanic event coeval with the PETM is also found in Kanthan and Kalakot area of the Jammu region (Shukla and Sharma, 2017, 2018; Siva Siddaiah and Shukla, 2012). Bhatia and Bhargava (2006) studied

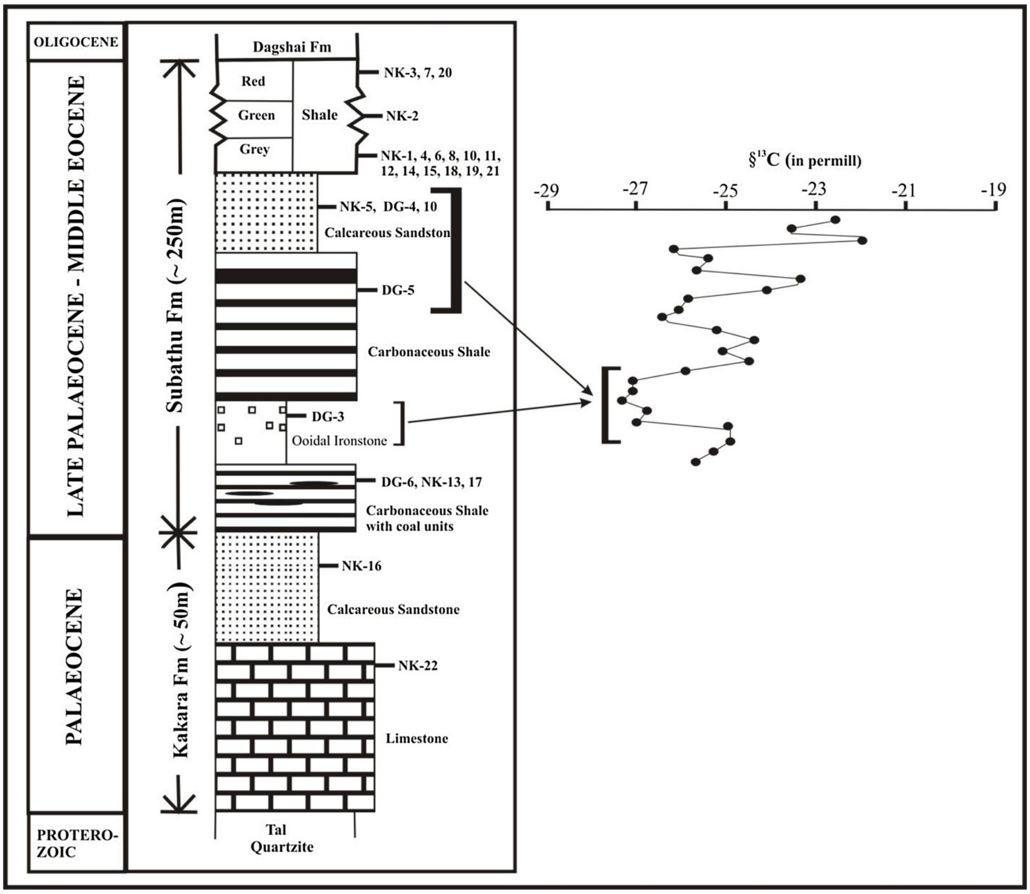

Fig. 2. Generalized Lithology of the study area with sample label and corresponding $\delta^{13}C$ values (modified after Siva Siddaiah, 2008).

biochronological continuity from the marine Subathu through Passage Beds (Late Lutetian to Middle Bartonian) to Dagshai and other equivalent Formations (Late Bartonian to Rupelian) of the Himalayan Foreland Basin.

The present study has been carried out to evaluate the Subathu Formation, explored at the Neelkanth (Lat/Long- 30°, 05′, 01″; 78°, 21′, 54″; Fig. 1) and Dogadda sections (Lat/Long- 29°, 48′, 20″; 78°, 35′, 49″) with respect to their geochemical characteristics, particularly, the stable carbon isotope ($\delta^{13}C$) and Rare-Earth Elements (REE) analyses. The REE's are successfully used by several workers to infer conditions of depositional environment (Piper and Bau, 2013; Song et al., 2014). The major objective of this study is to explore evidences of the Paleocene-Eocene warming event (PETM) using tropical hilly sediments as an archive and retrieve information through $\delta^{13}C$ and REE abundances.

2. Geological setting

The Subathu Formation (also known as Kakara-Subathu succession) occurs in foothills of the NW Himalaya (Fig. 2). They were formed during the Late Paleocene-Middle Eocene and have abundant and excellently preserved fauna fossils (Singh, 1980; Batra, 1989; Najman et al., 1997; Bajpai and Gingerich, 1998; Kumar and Kad, 2002). This formation is largely of shallow marine characteristics. However, conditions become continental towards the terminal end of the succession. It is underlain by the Kakara Formation of the Paleocene (Srikantia and Bhargava, 1967; Juyal and Mathur, 1990) comprised of limestone and calcareous sandstone. It is overlain by the terrestrial (or fluvial) sediments having an erosional contact with the Dagshai (ca. 31 ± 1.6 Ma) and Kasauli Formations of the Oligocene-Miocene (Najman et al., 1997; Najman and Garzanti, 2000; Najman et al., 2004; Bhatia and Bhargava, 2006; Bera et al., 2008, 2010). An unconformity of more than 10 Ma exists between the Subathu and the overlying Dagshai Formations (Najman et al., 2001, 2004; Bera et al., 2008).

The basement rock is the Precambrian Tal quartzite lying below the Kakara Formation. Thickness of the Subathu Formation (Kakara-Subathu succession) is about 250 m. It mainly consists of limestone, calcareous-sandstone, carbonaceous-shale with coal units and grey, green and red shales respectively occur from base to top (Fig. 2). Some channels of calcite veins (generally formed from shells of dead marine organisms) were found within the carbonaceous and grey shales (Fig. 3a and b), and they contain a little fraction of trace elements (e.g. Ti, Fe, Cu etc). The above mentioned individual litho-units can be grouped into three broad units i.e., black-grey unit at the bottom, grey-green unit in the middle part, and red-shale unit at the top of the Formation. The grey-green unit of the Subathu Formation is richly fossiliferous (Gastropoda, Ostracoda, Crocodilia, Pisces etc.). Its limestone unit yields oyster coquinites, a definite indicator of brackish water conditions that changed into fresh water conditions during the terminal deposition, i.e., the red-shale unit (Mathur, 1978; Juyal and Mathur, 1990; Mathur and Juyal, 2000). The red-shale unit at the top of the Subathu sediments, also referred as 'transitional or passage bed' is overlain by a marker horizon of orthoquartzitic sandstone between the Subathu and Dagshai Formations. The red-bed of upper Subathu Formation portrays a transitional environment from a marine set up to brackish, and subsequently to fluvial conditions (Kumar and Sahni, 1985; Bera et al., 2008). Interestingly, the stratigraphic position and characteristic properties of the Subathu Formation forms an ideal field laboratory to understand regional as well as global surface processes and the associated paleo-environmental implications.

Fig. 3. Field photographs of the a) Subathu shale with calcite veins; b) hand specimen of grey shale with calcite veins; c) Subathu shale at the Neelkanth section.

3. Methods and materials

The total 30 representative samples of Subathu Formation were collected from outcrops located at the Neelkanth (NK) and Dogadda (DG) sections (Fig. 3c) of Northwestern Himalaya (India). The stable carbon isotope ($\delta^{13}C$) analyses and total organic carbon (TOC) values were carried out on 25 samples following the method of Agrawal et al. (2017) at the Birbal Sahni Institute of Palaeosciences (BSIP), Lucknow. REE concentrations on 22 samples of the NK section were measured using an Inductively Coupled Plasma-Mass Spectrometry (Agilent 7700 series) hosted at BSIP. In order to measure REE, 100 mg of powdered sample was digested using a mixture of HF, HNO_3 and $HClO_4$ following the method described by Xiong et al. (2012). Reference standards [USGS (SGR1b and Sco1)] were used during the analysis. The precision was better than 5%. PAAS (McLennan, 2001) and average chondrite (Schmidt et al., 1963) values were used to normalize the REE pattern. Ce anomalies are traditionally calculated by comparing the normalized concentration of Ce ($[Ce]_n$) with its neighboring elements:

$$\text{Ce anomaly} = [2^*Ce_n]/[La_n + Pr_n]$$

Scanning Electron Microscopy (SEM) equipped with Energy-dispersive X-ray spectroscopy (Figs. 4 and 5) were used for determination

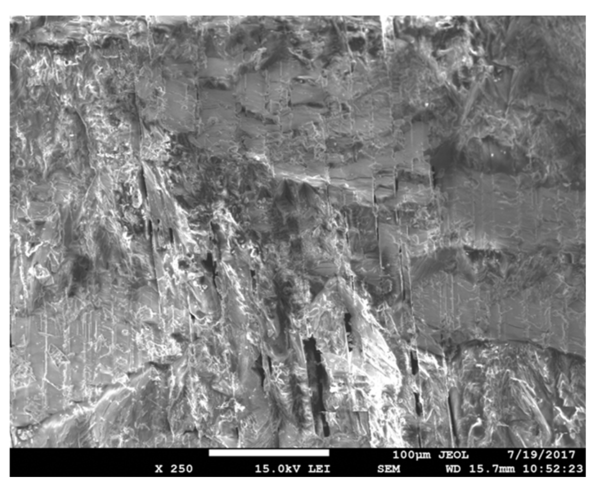

Fig. 4. Secondary electron (SE) images of the calcite veins.

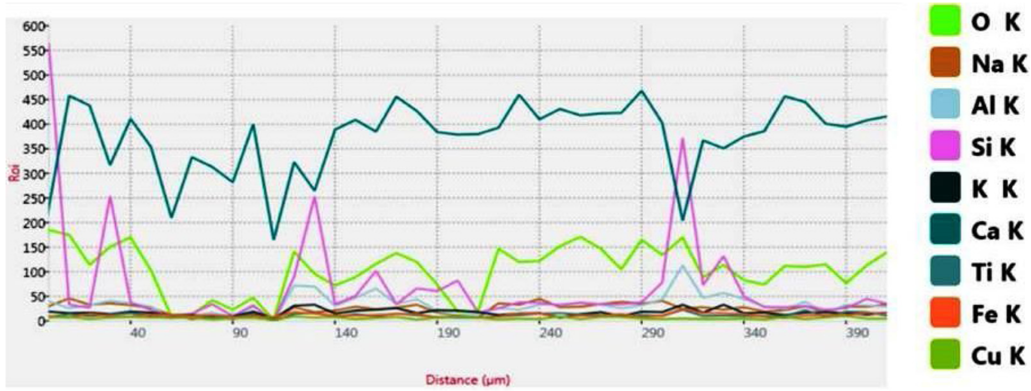

Fig. 5. Elemental distribution in calcite veins (EDX data, sample no.NK-10c).

Table 1
List of samples with their $\delta^{13}C$ and TOC values.

S.N	Sample No. (Top to Bottom)	$\delta^{13}C$ (per mill)	TOC (%)
1	NK3	−22.60	0.05
2	NK7	−23.5	0.02
3	NK20	−22.0	0.03
4	NK2	−26.10	0.07
5	NK1	−25.43	0.10
6	NK4	−25.59	0.73
7	NK6	−23.4	0.02
8	NK8	−24.08	0.27
9	NK10	−25.84	0.23
10	NK11	−26.03	0.14
11	NK12	−26.45	0.11
12	NK14	−25.21	0.16
13	NK15	−24.44	0.10
14	NK18	−25.12	0.14
15	NK19	−24.54	0.15
16	NK21	−25.91	0.09
17	**NK5**	**−27.05**	**0.04**
18	**DG4**	**−27.11**	**0.15**
19	**DG10**	**−27.34**	**0.04**
20	**DG5**	**−26.79**	**0.43**
21	**DG3**	**−26.97**	**0.80**
22	DG6	−24.96	2.39
23	NK9	−24.95	0.01
24	NK13	−25.33	0.17
25	NK17	−25.69	0.18

NK-Neelkanth (Lat/Long- 30°, 05′, 01″ ; 78°, 21′, 54″).
DG-Dogadda (Lat/Long- 29°, 48′, 20″ ; 78°, 35′, 49″).

of trace elements (e.g. Ti, Fe, Cu etc) present in calcite veins, at BSIP.

4. Results

$\delta^{13}C$ and total organic carbon (TOC) values are presented in Table 1. $\delta^{13}C$ values range from −22.0‰ to −27.34‰ and show about 5.3‰ variation. Five out of 25 samples (NK-5, DG-4, DG-10, DG-5, and DG-3 respectively from top to bottom; Fig. 2) show the carbon excursion values of about -27‰. Samples seats above and below this set of samples, have values of $\delta^{13}C$ are between -25‰ to -22.0‰. Samples NK-5, DG-4 and DG-10 are calcareous sandstone occupying the same stratigraphy, while samples DG-5 and DG-3 are carbonaceous shale and ooidal iron stone. TOC content in these five samples are low (< 0.80%), indicating highly oxidised depositional environment.

REE concentrations and related elemental ratios are listed in Table 2. The total REE abundance ranges from 27.23 ppm to 564.35 ppm with an average of 187.60 ppm. The 'Ce' concentration is quite high in all the samples as compare to other REE concentrations, with an average value of ~93 ppm. A few samples (e.g., NK-6, NK-20) contain > 250 ppm of 'Ce'. In most of the samples, the REE values (including Ce) are relatively close to values of the PAAS as compares to UCC. The much higher Ce concentration in samples NK-6 and NK-20, point towards maximum regression, occurred during their deposition. The chondrite and PAAS-normalized REE patterns of the samples are characterized by positive Ce anomaly. They are enriched in light rare-earth elements (LREE) and depleted in heavy rare-earth elements (HREE) with negative Eu anomaly (Figs. 6a, b and 7), subsequently indicating a felsic source as higher LREE/HREE ratios and negative Eu anomalies are generally found in felsic rocks. The Chondrite normalised diagram of grey-shale (NK-6) suits best with red-shale (NK-20; Fig. 6c), which indicates the same source of origin and depositional environment. Similarly the pattern of calcite veins (NK-12) perfectly matches with limestone (NK-22) proving its derivation from them (Fig. 6d). The overall 'Ce' anomaly (NK-1 to NK-21) ranges from 1.0 to 1.5, except one (NK-22) with anomaly of 4.45 value of 'Ce' anomaly (Fig. 8). Yttrium (Y) is often included with lanthanides due to having similar chemical properties to Holmium (Ho) (Tostevin et al., 2016a). The seawater generally displays high Y/Ho ratios (44–74), while the terrigenous materials and volcanic ash have uniform chondritic Y/Ho ratio of ~28 (Song et al., 2014). In the present case, Y/Ho ratios of Subathu samples range from ~30–45, which lies between the values of seawater and terrigenous materials (i.e., transition zone). The values of Y/Ho ratio have a good positive correlation with Y/Dy (Y/Dy = ~4.5–9; R^2 = 0.7; Fig. 9) and it indicates that they inherit shale-derived shallow marine characteristics.

The calcite veins present in some shale samples follow the same pattern of enriched LREE, depleted HREE and positive Ce-anomaly, along with the inclusion of redox sensitive trace elements (Ti, Fe and Cu) in the matrix (Figs. 4 and 5). The inclusion of redox sensitive trace elements in the matrix of calcite veins is generally due to increase in the temperature followed by the oxidized environment during their deposition. As a result of it, the cation exchange processes take place in which Ca (II) ions are replaced by the redox sensitive elements of similar ionic radii (e.g. Fe (II), Ti (II) and Cu (II) etc.)

5. Discussion

The oldest unit of the sub-Himalayan Paleogene succession, i.e., the Subathu Formation was largely marine (continental conditions towards its terminal stage). The overlying Formations i.e., the Dagshai and Kasauli are continental deposits (Najman and Garzanti, 2000; Kumar and Loyal, 2006; Bera et al., 2008, 2010). Most of the outcrops in the study area are disturbed (tectonically and structurally as well) and therefore it was difficult to find good exposures for extensive sedimentary logging and other geological analyses. However, we found some suitable exposures for collecting the representative samples in the Neelkanth and Dogadda sections of the study area. The basal rocks were deposited around 56 Ma which is also the approximate time of onset of the PETM, a well documented warming event studied worldwide.

Table 2
Rare-earth elements concentration (ppm) in sediments of Subathu Formation.

REE (PPM)	Sample no. NK-1 to 22										
	1	2	3	4	5	6	7	8	9	10	11
La	31.56	28.33	35.85	40.41	20.41	120.01	38.70	40.93	35.62	30.61	36.73
Ce	85.33	75.38	88.85	96.41	60.61	261.28	89.97	101.19	89.74	82.01	92.59
Pr	8.18	6.54	8.24	8.82	4.90	30.69	8.19	9.12	8.16	6.94	8.19
Nd	35.06	26.12	31.85	33.19	19.81	116.48	30.73	35.18	31.85	26.46	31.62
Sm	9.04	6.15	5.99	5.70	4.31	16.71	6.02	6.68	6.29	5.23	6.10
Eu	2.15	1.31	1.26	1.01	1.01	2.28	1.28	1.21	1.27	1.11	1.19
Gd	8.77	4.71	4.90	4.07	3.87	7.05	5.07	5.32	5.27	4.54	4.92
Tb	1.38	0.65	0.88	0.70	0.60	0.98	0.79	0.76	0.91	0.82	0.86
Dy	6.38	2.72	3.59	3.53	2.95	4.04	3.52	3.78	3.68	3.53	3.54
Ho	1.05	0.45	0.60	0.64	0.50	0.70	0.59	0.66	0.61	0.62	0.61
Er	2.60	1.23	1.60	1.87	1.34	1.95	1.55	1.80	1.56	1.66	1.63
Tm	0.31	0.16	0.21	0.26	0.18	0.26	0.20	0.25	0.20	0.21	0.22
Yb	1.82	1.05	1.27	1.72	1.09	1.68	1.28	1.54	1.21	1.37	1.34
Lu	0.24	0.14	0.17	0.23	0.15	0.23	0.17	0.21	0.16	0.18	0.18
Σ REE	193.89	154.95	185.25	198.56	121.73	564.35	188.06	208.63	186.52	165.31	189.70
Y	33.85	13.06	21.78	19.52	15.93	22.17	17.47	19.86	20.59	21.89	20.32
Y/Ho	32.34	28.75	36.12	30.29	31.81	31.72	29.37	30.08	33.73	35.46	33.53
Y/Dy	5.30	4.80	6.07	5.52	5.40	5.48	4.96	5.26	5.60	6.21	5.74
Ce/Ce*	1.17	1.21	1.13	1.11	1.33	0.95	1.09	1.14	1.15	1.23	1.16

REE (PPM)	12	13	14	15	16	17	18	19	20	21	22
La	7.90	31.21	42.94	11.54	14.11	35.08	26.27	16.21	81.24	28.04	1.99
Ce	32.17	80.77	106.91	47.01	49.79	90.13	73.20	46.79	241.25	68.74	20.65
Pr	2.46	6.74	9.15	2.73	3.63	7.59	5.72	3.81	29.62	5.87	0.53
Nd	12.86	25.93	35.02	11.38	15.83	28.86	22.13	15.60	129.06	21.49	2.10
Sm	5.57	5.19	6.48	2.97	4.32	5.49	4.45	3.54	29.43	4.26	0.42
Eu	1.87	1.11	1.23	1.06	1.10	1.15	1.07	0.88	5.38	0.85	0.10
Gd	6.25	4.39	5.29	2.92	4.35	4.71	3.91	3.46	14.44	3.91	0.45
Tb	0.98	0.69	0.84	0.41	0.79	0.80	0.63	0.59	1.26	0.70	0.08
Dy	3.92	3.27	3.96	2.05	3.16	3.46	2.82	2.64	3.90	3.44	0.37
Ho	0.57	0.56	0.68	0.34	0.52	0.60	0.48	0.45	0.59	0.65	0.08
Er	1.29	1.53	1.88	0.86	1.34	1.63	1.28	1.22	1.50	1.97	0.22
Tm	0.14	0.20	0.25	0.10	0.16	0.21	0.16	0.16	0.19	0.29	0.03
Yb	0.74	1.25	1.57	0.64	0.98	1.34	1.01	0.98	1.22	1.92	0.18
Lu	0.09	0.17	0.20	0.08	0.12	0.17	0.13	0.12	0.15	0.26	0.02
Σ REE	76.83	163.01	216.40	84.10	100.20	181.22	143.27	96.44	539.25	142.39	27.23
Y	24.84	17.57	21.87	11.96	23.66	20.90	16.25	16.91	18.04	21.87	3.25
Y/Ho	43.24	31.16	31.98	34.91	45.23	34.75	33.84	37.40	30.82	33.59	43.23
Y/Dy	6.33	5.37	5.53	5.83	7.49	6.04	5.76	6.41	4.62	6.36	8.73
Ce/Ce*	1.62	1.21	1.17	1.83	1.53	1.20	1.30	1.30	1.09	1.16	4.45

Represents the calculated Ce values to find Ce anomalies (Ce/Ce) in samples.

Therefore the basal rocks of the Subathu Formation may be helpful in providing inputs from the tropical regions (NW Himalaya), as most of the studies of PETM is documented from temperate regions of the world (Dickens et al., 2001; Crouch et al., 2003; Zachos et al., 2006, 2008; Bowen et al., 2015). It also furnishes information about terrestrial faunal link between India and Eurasia close to the Paleocene-Eocene transition (Smith et al., 2006).

The evidences in support of PETM/warming events have been found in different sedimentary sequences of India (Fig. 1). They are distributed along the NW Himalaya (e.g., Subathu's of Himanchal Pradesh, Jammu regions and Uttarakhand area (Siva Siddaiah and Kumar, 2007; Siva Siddaiah, 2008)), NE Himalaya (e.g., Meghalaya, Tewari et al., 2010; Srivastava and Prasad, 2015) and also from the western India (e.g., Gujarat, Samanta et al., 2013). Occurrence of the oldest volcanic ash bed reported from the basal part of the Subathu Formation from the NW Himalaya is an important evidence and indication of past warm interval equivalent to the PETM. Interestingly, the age of the PETM (~56.29 Ma) is also estimated from radiometric dates of marine ash layers (Westerhold et al., 2009). Its geological importance with respect to India-Asia collision and bearings on the Paleocene-Eocene boundary was discussed earlier (Acharyya, 2001; Huber et al., 2003; Siva Siddaiah and Kumar, 2007; Shukla and Sharma, 2017).

The stable carbon isotope ($\delta^{13}C$) data of the sediments of Subathu Formation shows an excursion of ~5‰ negative. The maximum excursion in $\delta^{13}C$ is noticed in calcareous sandstone of the basal section (DG-10) with value of −27.34‰, whereas the minimum excursion is observed with −22‰ in red Subathu (NK-20) occurring towards the terminal end. It may be coeval with the PETM warming episodes due to its equivalent stratigraphic position and characteristic analogue of CIE (~5–6‰) with the same.

The rare earth elements concentrations are not very high (avg. ~187 ppm). However, the 'Ce' concentration is relatively high in most of the samples. The chemical characteristic of Ce is unique due to its existence in both the +3 and +4 oxidation states. In highly oxic environment, Ce (III) is oxidized to insoluble Ce (IV) and its oxidation is catalyzed on the surface of Mn oxyhydroxides, as the standard reduction potential of Ce (IV) (+1.61 oV) is closer to Mn (IV) (+1.23 oV) (Tostevin et al., 2016b). The presence of a higher concentration of 'Ce' along with positive 'Ce' anomaly in the Subathu Formation clearly indicates a regressive phase and highly oxygenated environment of deposition, probably created due to the warming incidences happened in the geologic past. In the oxic conditions, 'Ce' is less readily dissolved in seawater, and enriched in the sediments with respect to the present context.

The overall geochemical characteristics of REE, positive 'Ce' anomaly and medium Y/Ho ratio indicate that depositional environment of the Subathu sediments was highly oxygenated and infected by the hydrothermal activity, probably due to the intense warming. These sediments were mostly shale-derived and deposited in a regressive phase of shallow marine environment. The stable carbon isotope ($\delta^{13}C$) values also suggest and support the intense warming period equivalent to PETM.

6. Conclusion

We suggest the following four outcomes from this study:

- Positive 'Ce' anomaly and dearth of TOC indicates highly oxygenated depositional environment for the Subathu Formation of the NW Himalaya.
- Presence of higher concentrations of REE and the chondrite normalized REE patterns indicate a felsic source, along with volcanic activity during that period, which subsequently was responsible for the rise of global temperature.
- The depositional setting and biostratigraphical constrained age along with negative Carbon Isotope Excursion values i.e. $\delta^{13}C$

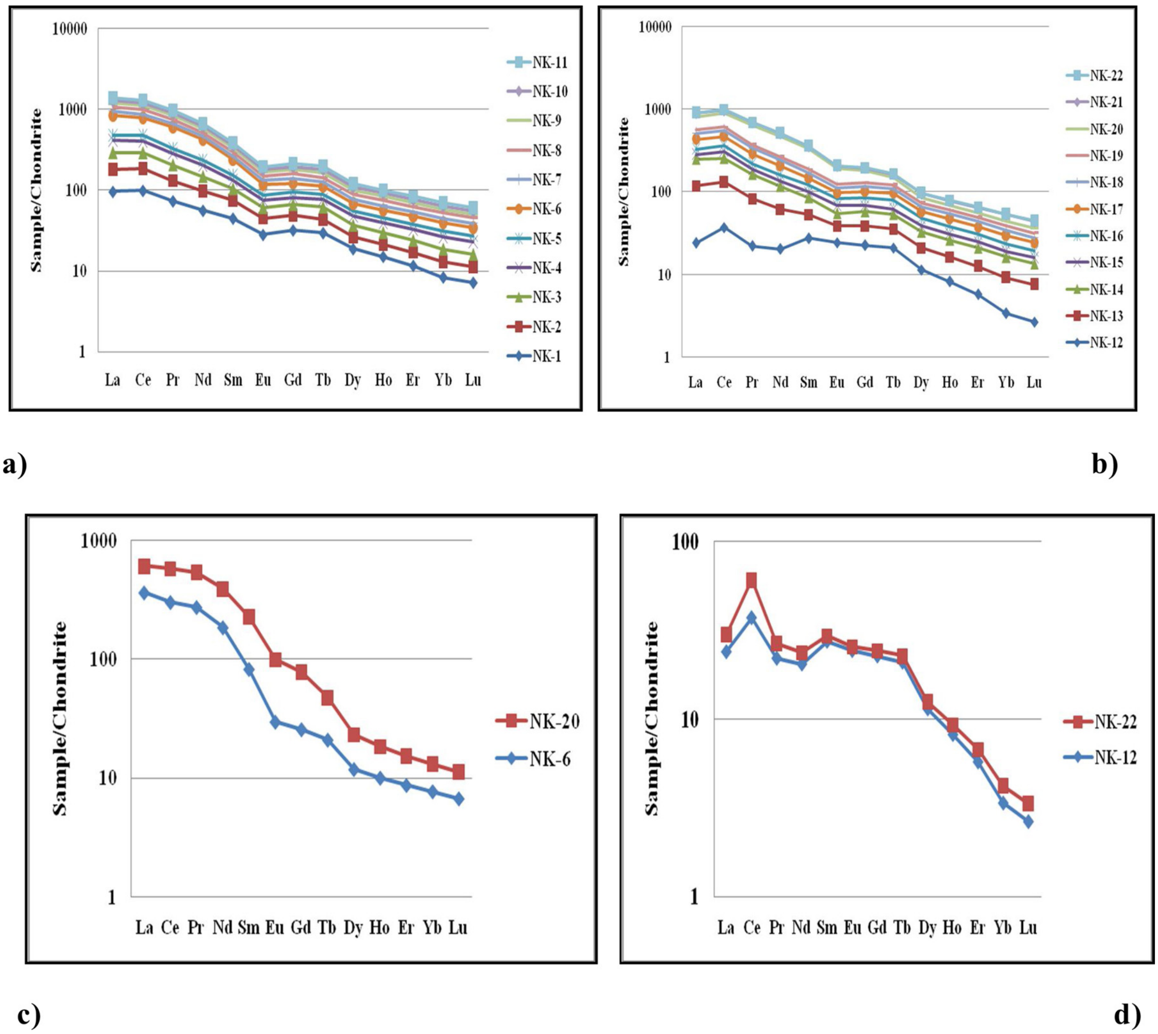

Fig. 6. Chondrite normalised diagram of Subathu sediments.
[a)-NK-1 to 11; b)- NK-12 to 22; c)- NK-6 (grey shale), NK-20 (red shale); d)- NK-12 (calcite veins); NK-22 (limestone)] (For interpretation of the references to colour in this figure legend, the reader is referred to the web version of this article).

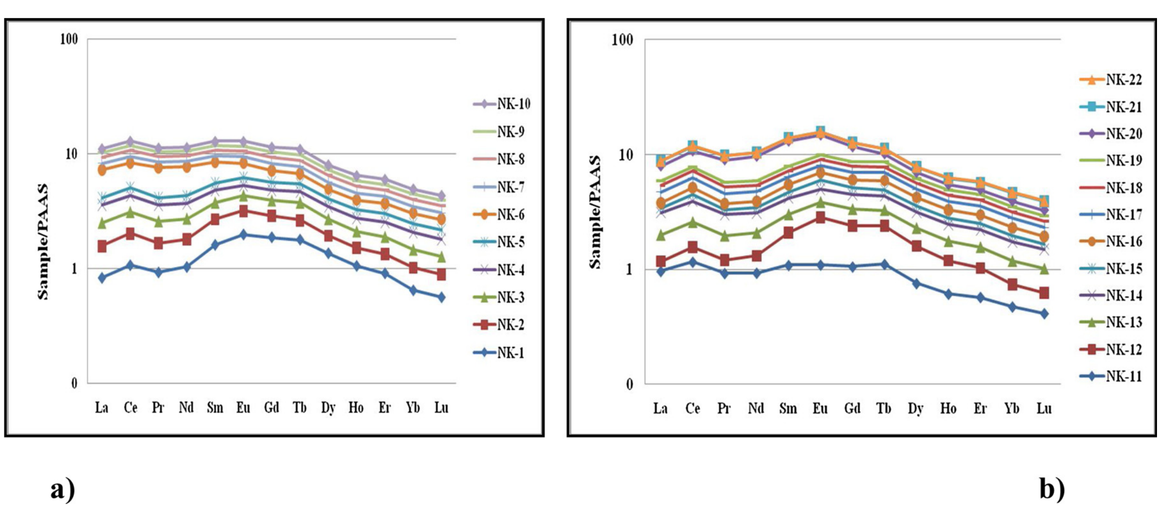

Fig. 7. PAAS normalised diagram of Subathu sediments [a)- NK-1 to 10, b)- NK-11 to 22].

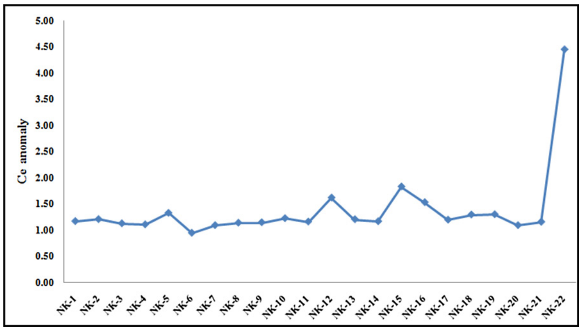

Fig. 8. Ce-anomaly diagram of Subathu sediments.

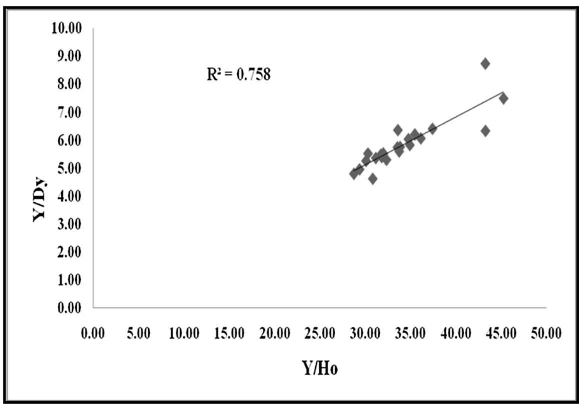

Fig. 9. Binary diagrtam of Y/Ho versus Y/Dy of Subathu sediments.

(~5.3‰) suggest that the Subathu Formation may be coeval with the Paleocene-Eocene Thermal Maxima (PETM) event.

- This study provides sedimentary archive of a modern analogue to understand the highly oxidized environment over paleo-tropical regions occurred during the Paleocene-Eocene.

Acknowledgements

MKS is thankful to SERB, Government of India for the financial support (File no. PDF/2015/00064) to this project. We express our sincere gratitude to the director BSIP for providing us necessary facilities. We are grateful to Dr Kamlesh Kumar for his help during field and Dr. Shailesh Agrawal and Dr. Pawan Govil for supporting in laboratory processes. We are indeed thankful to the editor and anonymous reviewers for their constructive remarks.

References

Acharyya, S.K., 2001. The role of India-Asia collision in the amalgamation of the Gondwana-derived blocks and deep-seated magmatism during the Paleogene at the Himalayan Foreland Basin and around the Gongha syntaxis in the south China block. Gondwana Res. 4 (1), 61–74.

Acharyya, S.K., 2007. Evolution of the Himalayan Paleogene foreland basin, influence of its litho-packet on the formation of thrust-related domes and windows in the Eastern Himalayas-a review. J. Asian Earth Sci. 31, 1–17.

Agrawal, S., Verma, P., Rao, M.R., Garg, R., Kapur, V.V., Bajpai, S., 2017. Lignite deposits of the Kutch Basin, western India: carbon isotopic and palynological signatures of the early Eocene hyperthermal event ETM2. J. Asian Earth Sci. 146, 296–303.

Bajpai, S., Gingerich, P.D., 1998. A new Eocene archaeocete (Mammalia: Cetacea) from India and the time of origin of whales. Proc. Natl. Acad. Sci. U. S. A. 95, 15464–15468.

Batra, R.S., 1989. A reinterpretation of the geology and biostratigraphy of the lower tertiary formations exposed along the Bilaspur-Shimla Highway, Himachal Pradesh, India. J. Geol. Soc. India 33, 503–523.

Bera, M.K., Sarkar, A., Chakraborty, P.P., Loyal, R.S., Sanyal, P., 2008. Marine to continental transition in Himalayan foreland. Geol. Soc. Am. Bull. 120, 1214–1232.

Bera, M.K., Sarkar, A., Tandon, S.K., Samanta, A., Sanya, P., 2010. Does burial diagenesis reset pristine isotopic compositions in paleosol carbonates? Earth Planet. Sci. Lett. 300, 85–100.

Bhatia, S.B., Bhargava, O.N., 2006. Biochronological continuity of the Paleogene sediments of the Himalayan Foreland Basin: paleontological and other evidences. J. Asian Earth Sci. 26, 477–487.

Bowen, G.J., Maibauer, B.J., Kraus, M.J., Röhl, U., Westerhold, T., Steimke, A., Gingerich, Philip D., Wing, S.C., Clyde, William C., 2015. Two massive, rapid releases of carbon during the onset of the Palaeocene-Eocene thermal maximum. Nat. Geosci. 8, 44–47.

Crouch, E.M., Dickens, G.R., Brinkhuis, H., Aubry, M.-P., Hollis, C.J., Rogers, K.M., Visscher, H., 2003. The Apectodinium acme and terrestrial discharge during the Paleocene-Eocene thermal maximum: new palynological, geochemical and calcareous nannoplankton observations at Tawanui, New Zealand. Palaeogeogr. Palaeoclimatol. Palaeoecol. 194, 387–403.

Dickens, G.R., et al., 2001. Carbon addition and removal during the Late Paleocene thermal maximum: basic theory with a preliminary treatment of the isotope record at ocean drilling program site 1051, Blake Nose. In: In: Kroon, D. (Ed.), Western North Atlantic Paleogene and Cretaceous Paleoceanography 183. Geol. Soc. Spec. Publ., pp. 293–305.

Huber, H., Koeberl, C., Egger, H., 2003. Geochemical study of lower Eocene volcanic ash layers from the alpine anthering formation, Austria. Geochem. J. 37, 123–134.

Juyal, K.P., Mathur, N.S., 1990. Ostracoda from the Kakara and Subathu formations of Himachal Pradesh and Garhwal Himalaya, India. J. Himal. Geol. 1 (2), 209–223.

Katz, M.E., Pak, D.K., Dickens, G.R., Miller, K.G., 1999. The source and fate of massive carbon input during the latest Paleocene thermal maximum. Science 286, 1531–1533.

Koch, P.L., Zachos, J.C., Dettmann, D.L., 1995. Stable isotope stratigraphy and paleoclimatology of the Paleogene Bighorn Basin (Wyoming, USA). Palaeogeogr. Palaeoclimatol. Palaeoecol. 115, 61–89.

Kumar, K., Kad, S., 2002. Early Miocene cricetid rodent (Mammalia) from the Murree Group of Kalakot, Rajauri District, Jammu and Kashmir, India. Curr. Sci. 82 (6), 736–740.

Kumar, K., Loyal, R.S., 2006. Excursion Guide on Sub-Himalayan Palaeogene Succession of Shimla Hills, for DST Sponsored National Field Workshop on Sub-Himalayan Palaeogene in the Context of India-Asia Collision (March 24–26, 2006).

Kumar, K., Sahni, A., 1985. Eocene mammals from the Upper Subathu Group, Kashmir Himalaya, India. J. Vertebr. Paleontol. 5 (2), 153–168.

Mathur, N.S., 1978. Biostratigraphical aspect of the Subathu Formation, Kumaun Himalaya. Recent Researches Geol. 5, 96–112.

Mathur, N.S., Juyal, K.P., 2000. Atlas of Early Palaeogene Invertebrate Fossils of the Himalayan Foothills Belt. Wadia Institute of Himalayan Geology Monogram Series, Bishen Singh, Mahendra Pal Singh, Dehradun.

McLennan, S.M., 2001. Relationships between the trace element composition of sedimentary rocks of upper continental crust. Geochem. Geophys. Geosyst. 2 (4), 1–24.

Najman, Y., Garzanti, E., 2000. Reconstructing early Himalayan tectonic evolution and paleogeography from tertiary foreland basin sedimentary rocks, northern India. Geol. Soc. Am. Bull. 112 (3), 435–449.

Najman, Y.M.R., Pringle, M.S., Johnson, M.R.W., Robertson, A.H.F., Wijbrans, J.R., 1997. Laser 40Ar/39Ar dating of single detrital muscovite grains from early foreland-basin sedimentary deposits in India: implications for early Himalayan evolution. Geology 25 (6), 535–538.

Najman, Y., Pringle, M., Godin, L., Oliver, G., 2001. Dating of the oldest continental sediments from the Himalayan foreland basin. Nature 410, 194–197.

Najman, Y., Johnson, K., White, N., Oliver, G., 2004. Evolution of Himalayan foreland basin, NW India. Basin Res. 16, 1–24.

Piper, D.Z., Bau, M., 2013. Normalized rare earth elements in water, sediments, and wine: identifying sources and environmental redox conditions. Am. J. Anal. Chem. 4, 69–83.

Samanta, A., Sarkar, A., Bera, M.K., Rai, J., Rathore, S.S., 2013. Late Paleocene-early Eocene carbon isotope stratigraphy from a near-terrestrial tropical section and antiquity of Indian mammals. J. Earth Syst. Sci. 122 (1), 163–171.

Schmidt, R.A., Smith, R.H., Lasch, J.E., Mosen, A.W., Olehy, D.A., Vasilevshis, J., 1963. Abundances of fourteen rare-earth elements, scandium, and yttrium in meteoritic and terrigenous matter. Geochim. Cosmochim. Acta 27 (6), 577–622.

Shukla, M.K., Sharma, A., 2017. Petrogenesis and mineral characteristics of the oldest volcanogenic breccia unit from the Himalayan Foreland Basin, India. GeoRes J. 13, 27–37.

Shukla, M.K., Sharma, A., 2018. A brief review on breccia: it's contrasting origin and diagnostic signatures. Solid Earth Sci. 3 (2), 50–59.

Singh, P., 1980. The Subathu Group of India. Prof. Paper, 1. Nav Jyoti Scientific Publications, Lucknow, pp. 1–89.

Singh, B.P., Tandon, S.K., Singh, G.P., Pawar, J.S., 2009. Palaeosols in early Himalayan foreland basin sequences demonstrate latitudinal shift-related long-term climatic change. Sedimentology 56, 1464–1487.

Siva Siddaiah, N., 2008. Berthierine-rich ooidal ironstone from the Late Palaeocene-Middle Eocene Subathu Formation, Dogadda area, NW Himalaya and its stratigraphic significance. Curr. Sci. India 94 (1), 123–127.

Siva Siddaiah, N., Kumar, K., 2007. Discovery of volcanic ash bed from the basal Subathu Formation (Late Palaeocene-Middle Eocene) near Kalka, Solan District (Himachal Pradesh), Northwest Sub-Himalaya, India. Curr. Sci. India 92, 118–125.

Siva Siddaiah, N., Shukla, M.K., 2012. Occurrence of rhyolite in Jangalgali Formation, Jammu and Kashmir, Northwest Himalaya, India. Curr. Sci. 103 (7), 817–821.

Smith, T., Rose, K.D., Gingerich, P.D., 2006. Rapid Asia-Europe–North America geographic dispersal of earliest Eocene primate *Teilhardina* during the Paleocene–Eocene thermal maximum. Proc. Nat. Acad. Sci. U. S. A. 103, 11,223–11,227.

Song, C., Herong, G., Linhua, S., 2014. Geochemical characteristics of REE in the Late Neo-proterozoic limestone from northern Anhui Province, China. Chin. J. Chem. 33, 187–193.

Srikantia, S.V., Bhargava, O.N., 1967. Kakara series–a new Paleocene formation in Simla

Hills. Bull. Geol. Soc. India 4 (4), 114–116.
Srivastava, J., Prasad, V., 2015. Effect of global warming on diversity pattern in Nypa mangroves across Paleocene-Eocene transition in the paleo-equatorial region of the Indian sub-continent. Palaeogeogr. Palaeoclimatol. Palaeoecol. 429, 1–12.
Tewari, V.C., Kumar, K., Lokho, K., Siddaiah, N.S., 2010. Lakadong limestone: Paleocene-Eocene boundaries carbonate sedimentation in Meghalaya, northeastern India. Curr. Sci. India 98 (1), 88–95.
Tostevin, R., Shields, G.A., Tarbuck, G.M., He, T., Clarkson, M.O., Wood, R.A., 2016a. Effective use of cerium anomalies as a redox proxy in carbonate-dominated marine settings. Chem. Geol. 438, 146–162.
Tostevin, R., Wood, R.A., Shields, G.A., Poulton, S.W., Guilbaud, R., Bowyer, F., Penny, A.M., He, T., Curtis, A., Hoffmann, K.H., Clarkson, M.O., 2016b. Low-oxygen waters limited habitable space for early animals. Nat. Commun. 7 (12818). http://dx.doi.org/10.1038/ncomms12818.
Westerhold, T., Rohl, U., McCarren, H.K., Zachos, J.C., 2009. Latest on the absolute age of the Paleocene-Eocene Thermal maximum (PETM): new insights from exact stratigraphic position of key ash layers .19 and .17. Earth Planet. Sci. Lett. 287, 412–419.
Xiong, Z., Li, T., Algeo, T., Chang, F., Yin, X., Xu, Z., 2012. Rare earth element geochemistry of laminated diatom mats from tropical West Pacific: evidence for more reducing bottom waters and higher primary productivity during the last glacial maximum. Chem. Geol. 296–297, 103–118.
Zachos, J.C., Pagani, M., Sloan, L.C., Thomas, E., Billups, K., 2001. Trends, rhythms, and aberrations in global climate 65 Ma to present. Science 292, 686–693.
Zachos, J.C., et al., 2006. Extreme warming of mid-latitude coastal ocean during the Paleocene-Eocene thermal maximum: inferences from TEX86 and isotope data. Geology 34, 737–740.
Zachos, J.C., Dickens, G.R., Zeebe, R.E., 2008. An early Cenozoic perspective on greenhouse warming and carbon-cycle dynamics. Nature 451, 279–283.